JJMIE

Volume 9 Number 2, April.2015
ISSN 1995-6665
Pages 75 - 84

Jordan Journal of Mechanical and Industrial Engineering

Controlling of Chaos Synchronization

Mohammad Ababneh *

Mechatronics Engineering Department, the Hashemite University, 13115 Zarqa, Jordan

Received 15 Feb 2015 *Accepted 29 March 2015*

Abstract

In the present paper, Linear Quadratic Regulator (LQR) and dual properties are employed to solve the observer-based synchronization problem. The synchronization is designed for nominal chaotic system, then it is applied to systems with uncertain parameters and systems with time-delays to investigate its tolerance to such systems. Moreover, to solve the nonlinear problem, which exist in chaotic systems, the optimal linearization technique is adopted to transform the nonlinear system into equivalent linear models. By linearizing the chaotic system and constructing linear models at every operating point, and then applying algebraic Riccati equation, the observer design problem is solved and chaotic synchronization is established. Numerical Simulations are used to demonstrate the effectiveness and feasibility of this design.

Keywords: *Chaos Synchronization, LQR, Observer Based Design, Chaotic Systems.*

1. Introduction

The investigation of chaos synchronization has been an active research topic in recent years [1-3]. Its applications are found in many engineering systems, such as mechanical systems, electromechanical systems, and industrial systems. For example, the Horizontal Platform System (HPS) is a mechanical system that exhibits rich chaotic dynamics and its synchronization was investigated in [4]. The drive and response systems were assumed to be disturbed by model uncertainties and external disturbances, the system parameters were assumed to be well-known. Using the update laws and the finite-time control theory, a robust adaptive controller was derived to synchronize the two uncertain systems in a finite time.

Furthermore, an adaptive synchronization method for a chaotic Permanent Magnet Synchronous Motor (PMSM) was developed in [5]. An adaptive synchronization method for a chaotic permanent magnet synchronous motor under model parameter variations was presented. Convergence of the closed-loop system responses was achieved by using a Lyapunov function.

Moreover, the synchronization and control of a chaotic supply chain management system was presented in [6]. The synchronization was performed using Lyapunov stability theory. And synchronization and control of chaotic supply chain management system were realized numerically.

Synchronization of chaos occurs when two systems adjust their motion to each other due to a coupling between them. It is important to highlight the relevance of chaos synchronization, especially in mechanical systems, optics and fluid dynamics. Furthermore, handling the parameter uncertainties and time delays is key element in the line of research. For example, in [7], Fourier series expansion and adaptive bounding technique were used to deal with periodical uncertainty. Using Lyapunov stability theory, the adaptive controller accomplished a hybrid function projective synchronization of a class of chaotic system with unknown time-varying parameters. Then using parameter updating laws, the nominal values of the unknown time-varying parameters were estimated.

However, in [8], only an adaptive bounding technique was used to handle such systems, where the master-slave synchronization problem of chaotic Lur'e systems was investigated. Only quantized sampled measurements were available for the controller. Using Lyapunov functional, an exponential asymptotical synchronization of master and slave system was achieved.

Moreover, in [9], the synchronization of chaos systems using fuzzy logic was addressed, where synchronization was achieved for uncertain nonlinear system with parameter uncertainties. The fuzzy modeling of chaotic systems using the Takagi-Sugeno (TS) model was used to provide many linearized systems for the nonlinear system under consideration. Then, the uncertainty decomposition was worked out by incorporating the uncertainties of the chaotic system in the fuzzy linear model. Where the uncertain chaotic system was expressed as set of linear models. Afterwards, an observer-based synchronization was performed for each linear model, and synchronization performed as the solution to a linear matrix inequality problem.

* Corresponding author. e-mail: ababneh@hu.edu.jo.

In all the studies mentioned above, complex mathematical models with computationally demanding approaches were required. Motivated by this reason, LQR method, which is a simpler and a more efficient method, was chosen for the present work [10, 11]. Therefore, the LQR and dual properties are employed to solve the observer-based synchronization problem from control point of view. And the chaos synchronization is applied to systems with uncertain parameters and systems with time-delays to investigate its tolerance to such systems. In order to highlight the advantage of this method, a comparison of its performance and the one's in [9] is made at the end of section 5.

The rest of the present paper is organized as follows. In section 2, the design of chaotic synchronized systems is presented. In section 3, the optimal linear method is discussed and the generation of linearized models around operating points is shown. In section 4, the linear quadratic control is discussed and the observer-based synchronization is derived. In Section 5, the effectiveness of the optimal linear model is demonstrated as simulation results, and discussion of these results is conducted in the same section. Finally, conclusions are presented in section 6.

2. Design of Chaotic Synchronized Systems

In the present paper, the observer approach is used to synchronize response system to drive system subjected to parameter uncertainties or time delays. Synchronization occurs when the states of the response system track the states of the drive system as time tends to infinity. Now, consider the following uncertain and time-delayed nonlinear drive system:

$$\begin{aligned} \dot{x}_c(t) &= f(x_c(t-t_0), \rho) \\ y_c(t) &= C(x_c(t-t_0), \rho) \end{aligned} \tag{1}$$

and a nominal nonlinear response system in the form:

$$\begin{aligned} \dot{\hat{x}}_c(t) &= \hat{f}(\hat{x}_c(t)) \qquad \hat{x}_c(0) = x_o \\ \hat{y}_c(t) &= C(\hat{x}_c(t)) \end{aligned} \tag{2}$$

where $f : \Re^n \to \Re^n$ and $\hat{f} : \Re^n \to \Re^n$ are nonlinear functions, $x_c(t) \in \Re^n$ $\hat{x}_c(t) \in \Re^n$ are the state vectors for the drive and response systems, $\rho \in \Re^p$ represents the parameter uncertainty and t_0 represents the delay time. Also, $y_c(t) \in \Re^n$ and $\hat{y}_c(t) \in \Re^n$ are the output vectors for the drive and response, respectively, and C is the constant output matrix.

There are many definitions of synchronization available in the literature; a working definition is to consider that the response system is synchronized to the drive system if the following criterion is satisfied [12]:

$$\lim_{t \to \infty} \left\| x(t) - \hat{x}(t) \right\| = 0 \tag{3}$$

The synchronization phenomenon may be viewed as an observer-design problem, and depending on the structure of the system, different approaches may be possible. Therefore, it is essential to have an observer-design, such that the error signal converges to zero globally and asymptotically, in this way the response is synchronized to the drive in the sense of equation (3). Noting that the chaotic systems in equations (1) and (2) are highly nonlinear, we shall introduce a technique for the linearization in the following section.

3. Optimal Linearization Method

Our approach in the present paper starts with Optimal Linearization Method (OLM) [13], in which a local linear model around every operating point of the system trajectory is obtained. Therefore, we deal with many linear models instead of one nonlinear model. Furthermore, OLM minimizes the modeling error between the original nonlinear system and its local linear model around each operating point of the system trajectory.

Now, consider a family of nonlinear systems of the form:

$$\dot{x}(t) = f(x(t)) + g(x(t))u(t) \tag{4}$$

where $f : \Re^n \to \Re^n$ and $g : \Re^n \to \Re^{n \times m}$ are smooth nonlinear functions, $x(t) \in \Re^n$ is the state vector, and $u(t) \in \Re^m$ is the control input.

Suppose that it is desired to find a linear model (A_j, B_j) around an operating point x_j, in the form:

$$\dot{x}(t) = A_j x(t) + B_j u(t) \tag{5}$$

with A_j and B_j being constant matrices of appropriate dimensions. One way to do this is to use the truncated Taylor expansion; however, if the operating point is not the origin, this will result in affine rather than a linear model. And in general the model is not local in both the state and the control terms.

The basic idea is to construct a local linear model, in both *x* and *u*, that approximates the dynamical behavior of the original nonlinear system in the vicinity of the operating state x_j; therefore, it is necessary to find two constant matrices, A_j and B_j, in the vicinity of operating point x_j such that the following two condition are satisfied:

$$f(x(t)) + g(x(t))u(t) \approx A_j x(t) + B_j u(t) \tag{6}$$

$$f(x_j) + g(x_j)u(t) = A_j x_j + B_j u(t) \tag{7}$$

Since the control input $u(t)$ is arbitrary, one should choose:

$$B_j = g(x_j) \tag{8}$$

So that equations (6) and (7) become quite simple:

$$f(x(t)) \approx A_j x(t) \tag{9}$$

and:

$$f(x_j) = A_j x_j . \tag{10}$$

Let a_i^T denotes the *ith* row of matrix A_j, then equations (9) and (10) can be rewritten as:

$$f_i(x(t)) \approx a_i^T x, \quad i = 1,2,...,n \tag{11}$$

and:

$$f_i(x_j) = a_i^T x_j, \quad i = 1,2,...,n, \tag{12}$$

where $f_i : \Re^n \to \Re^n$ is the *ith* row of function f. Then, expanding the left-hand side of equation (11) about x_j, and neglecting the second and higher order terms since they relatively small, we obtain:

$$f_i(x_j) + [\nabla f_i(x_j)]^T (x(t) - x_j) \approx a_i^T x(t) \tag{13}$$

where $\nabla f_i(x_j) : \Re^n \to \Re^n$ is the gradient column-vector of f_i evaluated at x_j. Using equation (12), one can rewrite equation (13) as:

$$[\nabla f_i(x_j)]^T (x(t) - x_j) \approx a_i^T (x(t) - x_j) \tag{14}$$

in which $x(t)$ is arbitrary state but should be close to x_j for a good approximation.

To determine a constant vector a_i^T such that it is close as much as possible to $\left[\nabla f_i(x_j)\right]^T$ and also satisfies $a_i^T x_j = f_i(x_j)$, we may consider the following constrained minimization problem:

$$\min \; E = \frac{1}{2}\left\|\nabla f_i(x_j) - a_i\right\|_2^2 \text{ subject to}$$

$$a_i^T x_j = f_i(x_j) \tag{15}$$

Notice that this is a convex constrained optimization problem. Therefore, the first order necessary condition for a minimization of E is also sufficient, which is:

$$\nabla_{a_i} E + \lambda \nabla_{a_i} (a_i^T x_j - f_i(x_j)) = 0 \tag{16}$$

where:

$$a_i^T x_j = f_i(x_j) \tag{17}$$

in which λ is the Lagrange multiplier and the subscript a_i in ∇_{a_i} indicates that the gradient is taken with respect to a_i. This then results in:

$$a_i - \nabla f_i(x_j) + \lambda x_j = 0, \tag{18}$$

By solving equation (18) with $x_j \neq 0$, this results in:

$$\lambda = \frac{x_j^T \nabla f_i(x_j) - f_i(x_j)}{\left\|x_j\right\|_2^2} x_j, \tag{19}$$

Substituting equation (19) into equation (18) for λ, for both $x_j \neq 0$ and $x_j = 0$, yields:

$$a_i = \begin{bmatrix} \nabla f_i(x_j) + \dfrac{f_i(x_j) - x_j^T \nabla f_i(x_j)}{\left\|x_j\right\|_2^2} x_j, & x_j \neq 0 \\ \nabla f_i(x_j), & x_j = 0 \end{bmatrix} \tag{20}$$

Note that equation (20) is the linearized systems taken at the operating points of the system trajectory. To this end, the subject of the present paper and the optimal linearization method have been introduced. In the following section, the LQR and observer-based synchronization is discussed.

4. Linear Quadratic Control

An important case of optimal control is the Linear Quadratic Regulator (LQR), where a measure of the quadratic continuous time cost function:

$$J = \tfrac{1}{2}\int_0^\infty \left[X^T(t) Q(t) X(t) + u^T(t) R(t) u(t)\right] dt \tag{21}$$

is minimized. Subject to linear dynamic constraints as given in the linearized models from the previous section, the Q and R matrices are positive definite matrices to ensure the cost measure remain positive. In addition, the negative feedback controller is in the form:

$$u(t) = -Kx(t) \tag{22}$$

It has been shown in optimal control theory that the feedback controller *K* is given by $K = R^{-1}B^T S$ where S is the solution of the well-known Algebraic Riccati equation[14]:

$$A^T S + SA - SBR^{-1}B^T S + Q = 0 \tag{23}$$

where *S* is symmetrical solution matrix. Note that the relationship between problem of state feedback controller and problem of observer design is duality relationship. In other words, both problems have similar solutions. Moreover, if we have a system of (*A*, *B*, *C*), then the system (A^T, C^T, B^T) is known as the dual system [15].

In general, the closed-loop system is given by:

$$\dot{x}(t) = (A - BK)x(t) \tag{24}$$

and the observer design is given by:

$$\dot{\hat{x}}(t) = A\hat{x}(t) - Bu(t) + L\left(y(t) - \hat{y}(t)\right) \tag{25}$$

and:

$$\hat{y}(t) = C\hat{x}(t) \tag{26}$$

where the *L* is observer matrix, then the error dynamics is $e(t) = \dot{x}(t) - \dot{\hat{x}}(t)$ and:

$$\dot{e}(t) = (A - LC)e(t). \tag{27}$$

We can clearly see that error dynamic of equation (27) is dual to closed loop system of:

$$AS_e + S_e A^T - S_e C^T R^{-1} C S_e + Q = 0 \tag{28}$$

where S_e is symmetrical solution matrix, and using duality property the observer matrix can be calculated as $L = S_e C^T R^{-1}$.

5. Simulation Results and Discussions

Observer-based synchronization is accomplished by forcing the error dynamics to zero as expressed in equation (3). This synchronization is performed for every linearized system A_j of equation (7) around every operating point x_j of the trajectory. In this section, simulation is implemented using two typical systems: Chua circuit and Chen system. The dimensionless form of Chua circuit is obtained as [16]:

$$\begin{aligned} \dot{x}_1(t) &= \alpha\left[x_2(t) - x_1(t) - g_{NL}(x_1(t))\right] \\ \dot{x}_2(t) &= x_1(t) - x_2(t) + x_3(t) \\ \dot{x}_3(t) &= -\beta x_2(t) \end{aligned} \tag{29}$$

where $g_{NL}(x_1(t)) = m_2 x_1(t) + m_3 x_1(t)^3$. The system has a complex attractor with nominal parameters $\alpha = 9, \beta = (14\frac{2}{7}), m_2 = -5/7, m_3 = -8/7$.

Referring back to section 3, the OLM for the Chua's linearized system was calculated as:

$$A_j \begin{cases} \begin{bmatrix} \alpha(m_2-1) - 3\alpha m_3 x_1^2 + \dfrac{2\alpha m_3 x_1^4}{\|x_j\|_2^2} & \alpha + \dfrac{2\alpha m_3 x_1^3 x_2}{\|x_j\|_2^2} & \dfrac{2\alpha m_3 x_1^3 x_3}{\|x_j\|_2^2} \\ 1 & -1 & 1 \\ 0 & -\beta & 0 \end{bmatrix} & for \ \|x_j\|_2^2 \neq 0 \\ \begin{bmatrix} \alpha(m_2-1) - 3\alpha m_3 x_1^2 & \alpha & 0 \\ 1 & -1 & 1 \\ 0 & -\beta & 0 \end{bmatrix} & for \ \|x_j\|_2^2 = 0 \end{cases} \quad (30)$$

After finding the linearized model, the drive state vector $\begin{bmatrix} x_1 & x_2 & x_3 \end{bmatrix}^T$ and its synchronized drive states vector $\begin{bmatrix} \hat{x}_1 & \hat{x}_2 & \hat{x}_3 \end{bmatrix}^T$ were found using equations (24) and (25), the synchronization was performed using Matlab ® with a Runge Kutta fourth-order algorithm, with a fixed integration step $\tau = 0.005$ seconds. At first, the synchronization was performed for nominal case without uncertainty and without time delay, and the simulation is shown in Figure 1, with excellent synchronization performance where response states follow drive states perfectly when time passes. Then time varying parameters uncertainties were introduced in the drive system as following:

$\alpha + \Delta\alpha = (9)(1 + \zeta \sin(10t))$,

$\beta + \Delta\beta = (14\frac{2}{7})(1 + \zeta \sin(10t))$,

and

$m_2 + \Delta m_2 = (\frac{-5}{7})(1 + \zeta \sin(10t))$,

$m_3 + \Delta m_3 = (\frac{-8}{7})(1 + \zeta \sin(10t))$,

where ζ is the percentage uncertainty. Then, nominal synchronization is applied to this uncertain drive and its performance is shown in Figure 2 with $\zeta = 10\%$; the response shows some deterioration especially in X_2 state. To better understand the effect of uncertainty, a measure of performance was introduces as follows:

$$\sum_{j=1}^{3} \sum_{i=1}^{n} \left(\frac{|x_i(t) - \hat{x}_i(t)|}{n} \right)_j \quad (31)$$

where i represents the operating point and j represents the trajectory, the tracking error for all points at increasing uncertainties in all three trajectories were taken, and then summed, averaged by the total number of sampling points, and recorded in Table 1. Note the measure worsening with the increasing of parameter uncertainty, where, roughly, the measure doubled with a small increase of uncertainty. Normalizing the measure by dividing the measures by the maximum range of trajectories, gives a better understating of the changes subjected to increasing parameter uncertainty as shown in Table 1. Note that 'the maximum range of trajectories' is the difference between the maximum value and the minimum value of the drive trajectories' points

A similar action was taken with time delay system, where the nominal synchronization was applied to the time delayed drive; the synchronization performance is shown in Figure 3 for 0.2 second delay. The delay of about 0.2 seconds was obvious in all trajectories; however, if the effect of delay is neglected, it is noted that the response states follow the drive states closely. Table 2 records the measures and normalized measures that were explained above; these readings show that the measures worsen with the increase of the delay at a steady rate.

The second typical chaotic system is Chen system which is expressed as [17]:

$$\begin{bmatrix} \dot{x}_1(t) \\ \dot{x}_2(t) \\ \dot{x}_3(t) \end{bmatrix} = \begin{bmatrix} a & (x_2(t) - x_1(t)) \\ (c-a) & x_1(t) - x_1(t)x_3(t) + c\,x_2(t) \\ x_1(t)x_2(t) - b & x_3(t) \end{bmatrix} \quad (32)$$

The system has a complex attractor with nominal parameters $a = 35, b = 3, c = 28$. Referring back to section 3, the OLM for the Chen linearized system was calculated as:

$$A_j \begin{cases} \begin{bmatrix} -a & a & 0 \\ c-a-x_{j3}+\dfrac{x_{j1}^2 x_{j3}}{\|x_j\|_2^2} & c+\dfrac{x_{j1}x_{j2}x_{j3}}{\|x_j\|_2^2} & -x_{j1}+\dfrac{x_{j1}x_{j3}^2}{\|x_j\|_2^2} \\ x_{j2}-\dfrac{x_{j1}^2 x_{j2}}{\|x_j\|_2^2} & x_{j1}-\dfrac{x_{j1}x_{j2}^2}{\|x_j\|_2^2} & -b-\dfrac{x_{j1}x_{j2}x_{j3}}{\|x_j\|_2^2} \end{bmatrix} & for \quad \|x_j\|_2^2 \neq 0 \\ \begin{bmatrix} -a & a & 0 \\ c-a-x_{j3} & c & -x_{j1} \\ x_{j2} & x_{j1} & -b \end{bmatrix} & for \quad \|x_j\|_2^2 = 0 \end{cases} \tag{33}$$

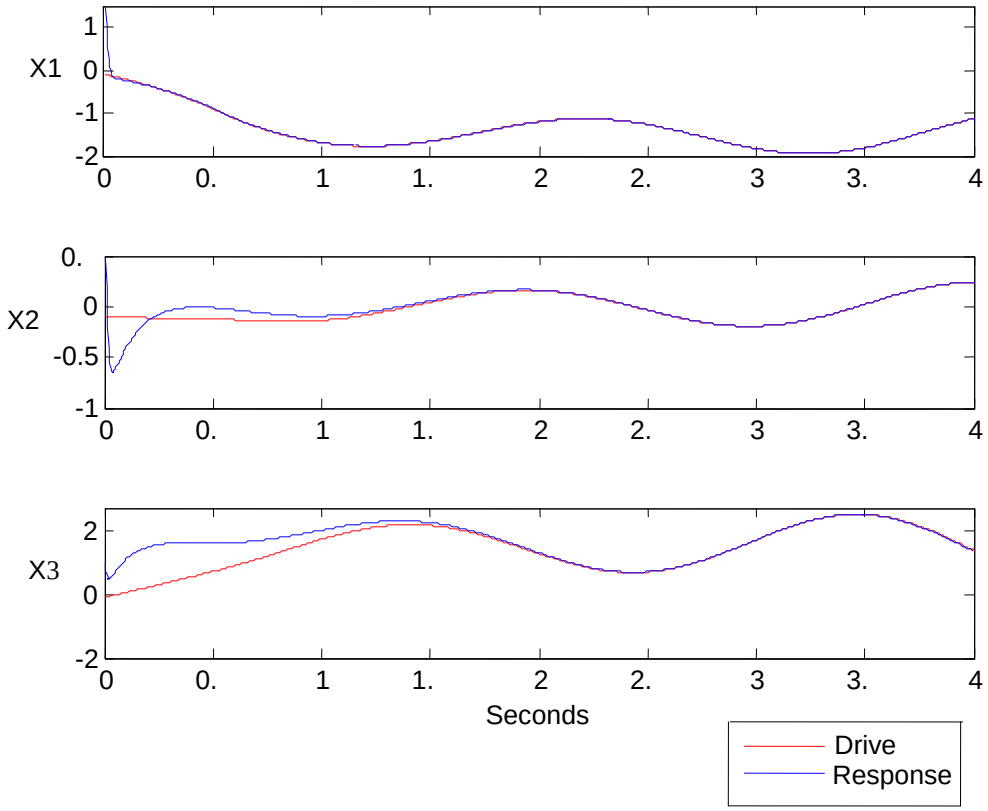

Figure 1. Nominal Chua's circuit synchronization

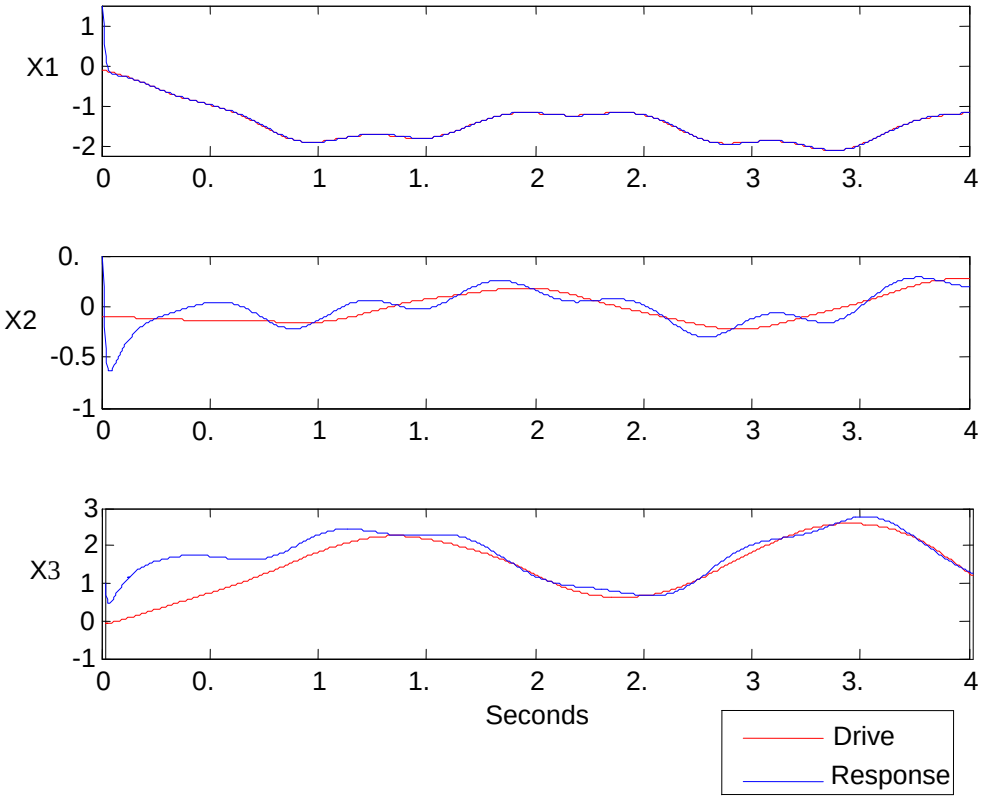

Figure 2. Chua's circuit synchronization with $\zeta = 10\%$

Table 1. Chua circuit synchronization subjected to increasing uncertainty

Type	Nominal	10%	20%	30%	40%	50%	60%
Measure	0.0094	0.0132	0.0196	0.0311	0.0499	0.0796	0.1287
Normalized Measure	0.0021	0.0030	0.0044	0.0070	0.0112	0.0179	0.0289
Type	70%	80%	90%	100%	110%	120%	200%
Measure	0.2209	0.4738	1.9272	16.5683	203.7033	30181	$3.2*10^{17}$
Normalized Measure	0.0496	0.1065	0.4331	3.7235	45.7801	6782.9	$7.2*10^{17}$

Table 2. Chua's circuit synchronization subjected to increasing time delay

Delay	Nominal	0.025 sec	0.050 sec	0.075 sec	0.1 sec	0.2 sec	0.3 sec
Measure	0.0094	0.0668	0.0967	0.1266	0.1563	0.2764	0.3949
Normalized Measure	0.0021	0.0150	0.0217	0.0285	0.0351	0.0621	0.0887
Delay	0.4 sec	0.5 sec	0.6 sec	0.7 sec	0.8 sec	0.9 sec	1.0 sec
Measure	0.5065	1.8261	0.6993	0.7759	0.8376	0.8839	0.9145
Normalized Measure	0.1138	0.4104	0.1572	0.1744	0.1882	0.1986	0.2055

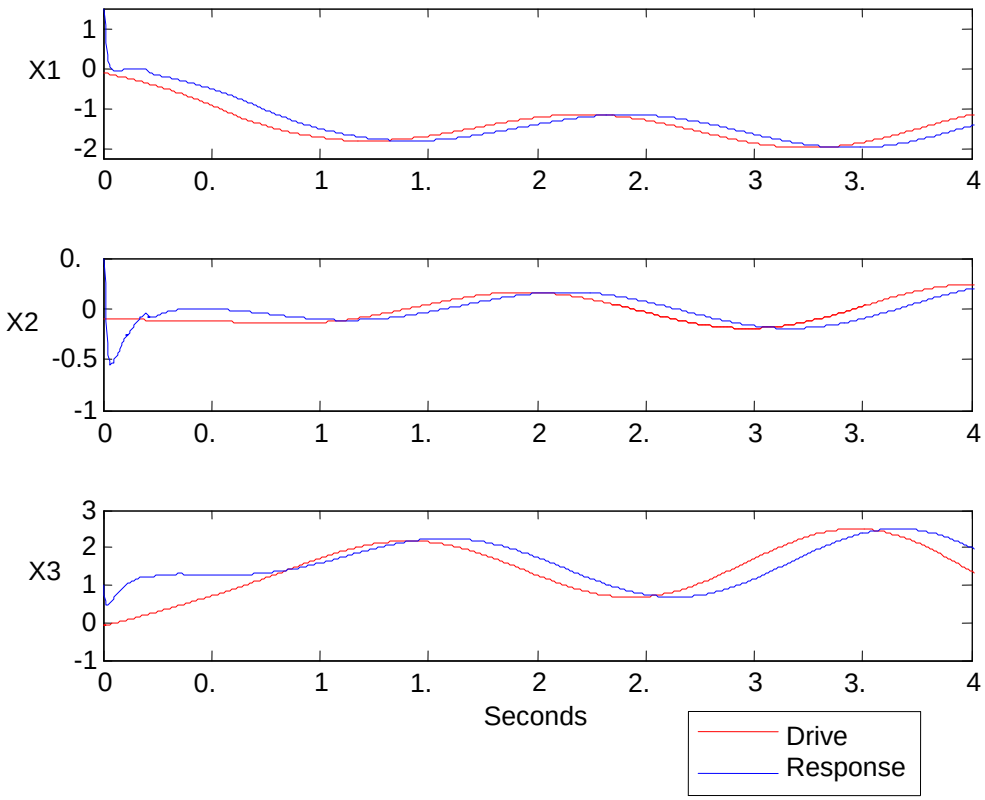

Figure 3.Chua's circuit synchronization subjected to a 0.2 second delay

Now, the drive state vector $\begin{bmatrix} x_1 & x_2 & x_3 \end{bmatrix}^T$ and its synchronized drive states vector $\begin{bmatrix} \hat{x}_1 & \hat{x}_2 & \hat{x}_3 \end{bmatrix}^T$ were found using equations (24) and (25), the synchronization was performed using Matlab ® with a Runge Kutta fourth-order algorithm, with a fixed integration step $\tau = 0.005$ seconds. At first the synchronization was performed for nominal case without uncertainty neither time delay, and the simulation is shown in Figure 4, with excellent synchronization performance were response states follow drive states perfectly when time elapses. Then time varying parameters uncertainties were introduced in the drive system as following:

$$b + \Delta b = (3)(1 + \zeta \sin(10t)),$$
$$a + \Delta a = (35)(1 + \zeta \sin(10t))$$
$$c + \Delta c = (28)(1 + \zeta \sin(10t)),$$

where ζ is the percentage uncertainty. And nominal synchronization applied to this uncertain drive and its performance is shown in Figure 5 with $\zeta = 30\%$, the response shows some deterioration; however, it was noted that the Chen system performed much better than the Chua circuit at low parameter uncertainties. And this is clear when comparing Table 1 with Table 3. To better understand the effect of uncertainty, a measure of performance for increasing uncertainties was recorded in Table 3. Note the measure worsening with the increase of parameter uncertainty at a steady rate, then reach the instability at $\zeta = 170\%$. Normalizing the measure, as explained above, gives a better understating of the changes subjected to the increase of parameter uncertainty as shown in Table 3, where the normalized measure was relatively low for $\zeta \leq 100\%$.

A similar action was taken with time delay system, where the nominal synchronization is applied to the time delayed drive; the synchronization performance is shown in Figure 6 for 0.2 second delay. The delay of about 0.2 seconds was obvious in all trajectories; however, if the effect of the delay is neglected, the response states follow the drive states closely, and this is similar to the performance in Chua circuit. Table 4 records the measures and normalized measures that were explained above; the measures worsen with the increase of the delay. However, the measure after 0.5 seconds started to fluctuate by decreasing then increasing; this is due to the distortion in the response signal because of the significant delay; it is also due to the fast dynamics of the Chen system.

Comparing this method with other methods, as the one in [9], will highlight the advantage of this method. The Chua circuit with parameter uncertainties was chosen to perform the comparison. As recorded in Table 5 below, most of the cases of parameter uncertainties shown a better performance in this method than the one in [9]. Therefore, this indicates the efficiency of this method.

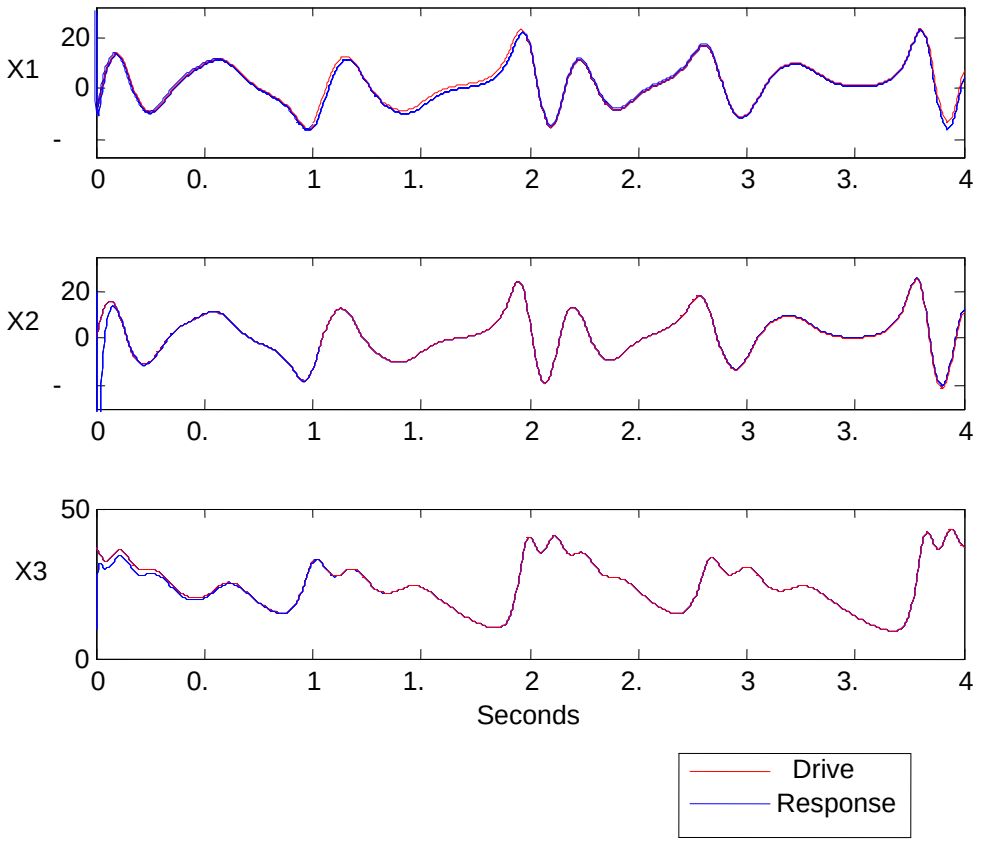

Figure 4. Nominal Chen circuit synchronization

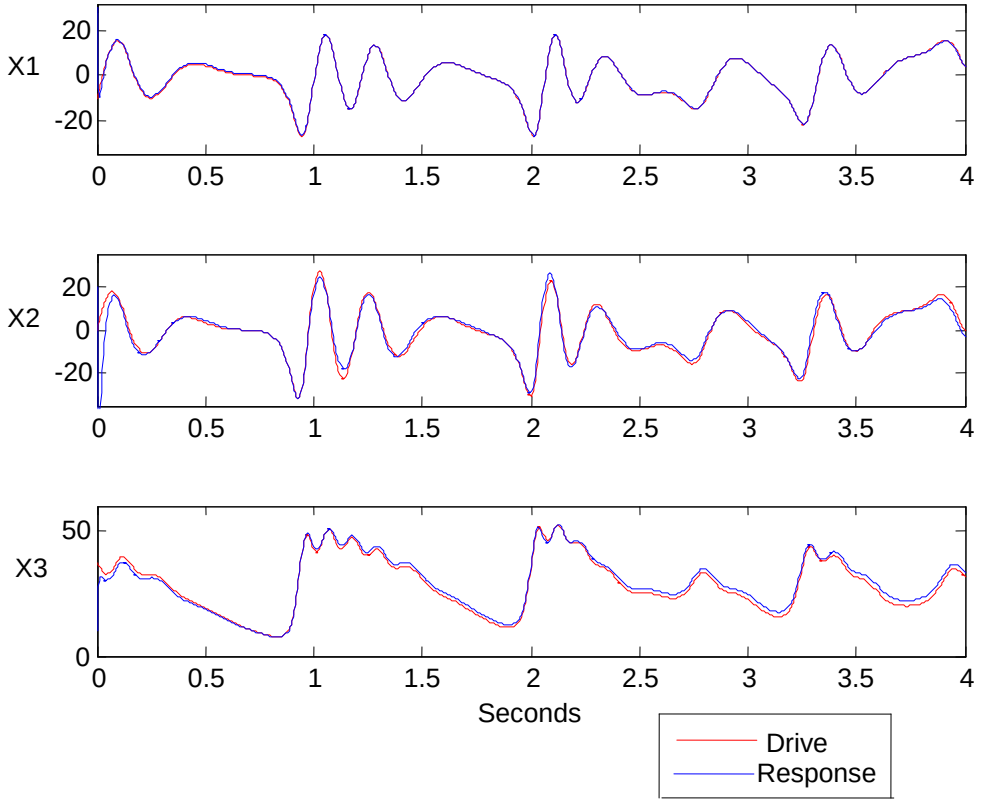

Figure 5. Chen system synchronization with $\zeta = 30\%$

Table 3. Chen system synchronization subjected to increasing parameter uncertainty

Type	Nominal	10%	20%	30%	40%	50%	60%
Measure	0.2759	0.4717	0.7152	1.0069	1.3231	1.5804	1.7853
Normalized Measure	0.0044	0.0075	0.0113	0.0159	0.0209	0.0250	0.0282
Type	70%	80%	90%	100%	120%	120%	170%
Measure	2.2912	2.8243	3.1203	3.8673	6.9852	12.5255	unstable
Normalized Measure	0.0362	0.0447	0.0494	0.0612	0.1105	0.1982	unstable

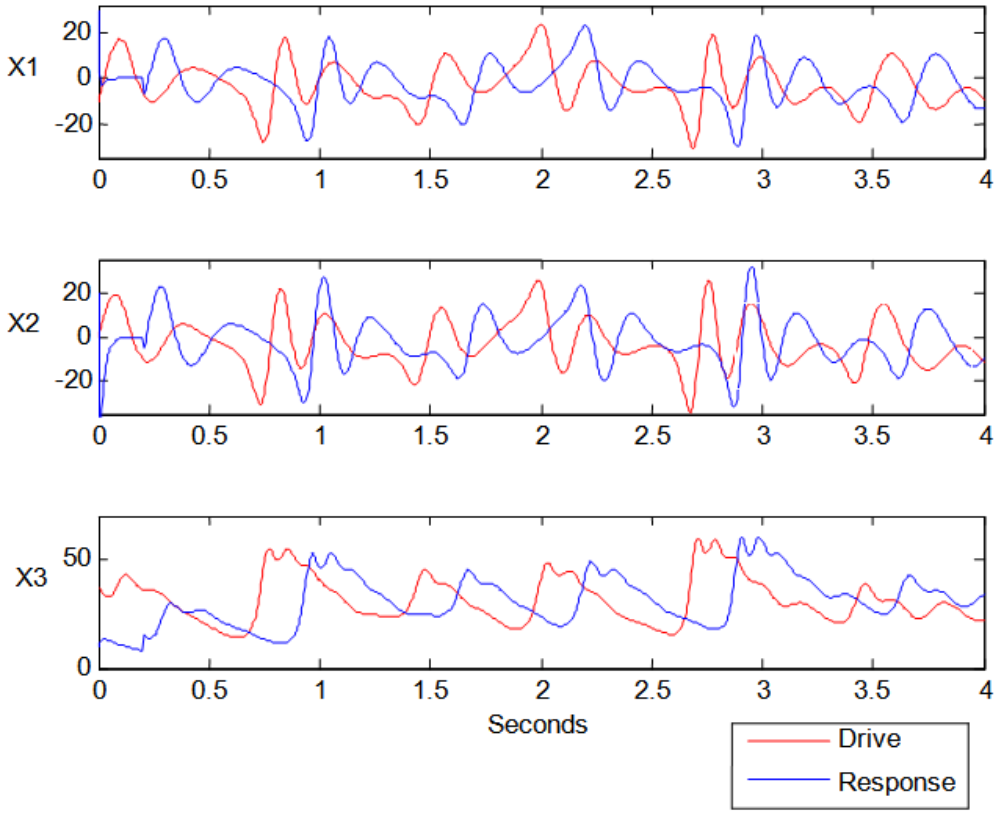

Figure 6. Chen system synchronization subjected to a 0.2 second state-delay

Table 4. Chen system synchronization subjected to increasing time delay

Delay	Nominal	0.025 sec	0.050 sec	0.075 sec	0.1 sec	0.2 sec	0.3 sec
Measure	0.2759	4.5415	7.5047	9.8771	11.6318	13.2562	13.8022
Normalized Measure	0.0044	0.0718	0.1187	0.1563	0.1840	0.2097	0.2184
Delay	0.4 sec	0.5 sec	0.6 sec	0.7 sec	0.8 sec	0.9 sec	1.0 sec
Measure	14.0187	12.7388	11.9915	11.1585	12.6575	14.3675	14.1958
Normalized Measure	0.2218	0.2015	0.1897	0.1765	0.2003	0.2273	0.2246

6. Conclusions

A design of observer-based synchronization of chaotic system was developed in the present paper. It is based on state feedback LQR and duality property to solve the observer design. This synchronization is simple to design and proved to withstand significant parameter uncertainties and a state delay. A performance measure was introduced to demonstrate system performance under increasing parameter uncertainties and state delays. The effectiveness and feasibility of such a design were simulated in Matlab ® and discussed for two benchmark systems, the Chua circuit and the Chen system. A large number of cases for both increasing parameter uncertainties cases and increasing time-delayed cases was conducted, then the performance of these cases is recorded in the tables above to demonstrate the performance trends for such systems.

References

[1] Y. J. Sun, "A novel chaos synchronization of uncertain mechanical systems with parameter mismatchings, external excitations, and chaotic vibrations". Communications in Nonlinear Science and Numerical Simulation, Vol. 17 (2012), Issue 2, 496-504.

[2] M.R. Faieghi, S.K. Mashhadi, D. Baleanu, "Sampled-data nonlinear observer design for chaos synchronization: A Lyapunov-based approach". Communications in Nonlinear Science and Numerical Simulation, Vol. 19 (2014), Issue 7, 2444-2453.

[3] Y. Chen, X. Wu, Z. Liu, "Global chaos synchronization of electro-mechanical gyrostat systems via variable substitution control". Chaos, Solitons & Fractals, Vol. 42 (2009), Issue 2, 1197-1205.

[4] M.P. Aghababa, H.P. Aghababa, "Synchronization of mechanical horizontal platform systems in finite time". Applied Mathematical Modelling, Vol. 36 (2012), Issue 10, 4579-4591.

[5] S.S. Kim, H.H. Choi, "Adaptive synchronization method for chaotic permanent magnet synchronous motor". Mathematics and Computers in Simulation, Vol. 101 (2014), 31-42.

[6] A. Göksu, U. Kocamaz,Y. Uyaroğlu, "Synchronization and control of chaos in supply chain management". Computers & Industrial Engineering, In Press, Corrected Proof, Available online (2014).

[7] C. Zhan, J. Li, "Hybrid Function Projective Synchronization of Chaotic Systems with Uncertain Time-varying Parameters Fourier Series Expansion". International Journal of Automation and Computing , Vol. 9 (2012), Issue 4, 388-394.

[8] X. Xiao, L. Zhou, Z. Zhang, "Synchronization of chaotic Lur'e systems with quantized sampled-data controller". Communications in Nonlinear Science and Numerical Simulation, Vol. 19 (2014), Issue 6, 2039-2047.

[9] M. Ababneh, I. Etier, M. Smadi and J. Ghaeb, " Synchronization of Chaos Systems Using Fuzzy Logic," Journal of Computer Science, vol. 7 (2011), pp. 197-205.

[10] L. Chrif, Z. Kadda, "Aircraft Control System Using LQG and LQR Controller with Optimal Estimation-Kalman Filter Design", Procedia Engineering, Vol. 80 (2014), 245-257.

[11] S. Schulz, H. Gomes, A. Awruch, "Optimal discrete piezoelectric patch allocation on composite structures for vibration control based on GA and modal LQR". Computers & Structures, Vol. 128 (2013), 101-115.

[12] A. Senouci, A. Boukabou, "Predictive control and synchronization of chaotic and hyperchaotic systems based on a T–S fuzzy model" Mathematics and Computers in Simulation, Vol. 105 (2014), 62-78.

[13] M. Ababneh, M. Salah, K. Al-Widyan, " Linearization of nonlinear dynamical system: A comparative study ". Jordan Journal of Mechanical and Industrial Engineering, Vol. 5 (2011), 567 - 571.

[14] Z. Ulukök, R. Türkmen, "Improved upper bounds for the solution of the continuous algebraic Riccati matrix equation". Applied Mathematics and Computation, Vol. 225, (2013), 306-317.

[15] Ostertag E, Mono and Multivariable Control and Estimation: Linear, Quadratic and LMI Methods. 2011 edition. Berlin: Springer; 2011.

[16] E. Ponce, J. Ros, E. Vela, "Unfolding the fold-Hopf bifurcation in piecewise linear continuous differential systems with symmetry". Physica D: Nonlinear Phenomena, Vol. 250 (2013Y, 34-46.

[17] S. Das, A. Acharya, I. Pan, "Simulation studies on the design of optimum PID controllers to suppress chaotic oscillations in a family of Lorenz-like multi-wing attractors". Mathematics and Computers in Simulation, Vol. 100 (2014), 72-87.